tvst

Retina

Role of Hsa_circ_0000880 in the Regulation of High Glucose-Induced Apoptosis of Retinal Microvascular Endothelial Cells

Jiawei Wang[1,*], Nannan Yang[1,2,*], Wanna Li[1], Han Zhang[3], and Jianqiao Li[1]

[1] Department of Ophthalmology, Qilu Hospital, Cheeloo College of Medicine, Shandong University, Jinan, China
[2] Department of Ophthalmology, The People's Hospital of Laoling City, Dezhou, Shandong, China
[3] Department of Ophthalmology, Shandong Provincial Hospital Affiliated to Shandong First Medical University, Jinan, China

Correspondence: Jianqiao Li, Department of Ophthalmology, Qilu Hospita, Cheeloo College of Medicine, Shandong University, Jinan 250033, China. e-mail: 18560087118@163.com
Han Zhang, Department of Ophthalmology, Shandong Provincial Hospital Affiliated to Shandong First Medical University, Jinan 250033, China. e-mail: han11_zhang@163.com

Received: December 13, 2023
Accepted: March 12, 2024
Published: April 8, 2024

Keywords: circular RNA (circRNA); EIF4A3; diabetic retinopathy (DR); retinal microvascular endothelial cell (RMEC)

Citation: Wang J, Yang N, Li W, Zhang H, Li J. Role of hsa_circ_0000880 in the regulation of high glucose-induced apoptosis of retinal microvascular endothelial cells. Transl Vis Sci Technol. 2024;13(4):12, https://doi.org/10.1167/tvst.13.4.12

Purpose: Circular RNAs (circRNAs) have been verified to participate in multiple biological processes and disease progression. Yet, the role of circRNAs in the pathogenesis of diabetic retinopathy (DR) is still poorly understood and deserves further study. This study aimed to investigate the role of circRNAs in the regulation of high glucose (HG)-induced apoptosis of retinal microvascular endothelial cells (RMECs).

Methods: Epiretinal membranes from patients with DR and nondiabetic patients with idiopathic macular epiretinal membrane were collected for this study. The circRNA microarrays were performed using high-throughput sequencing. Hierarchical clustering, functional enrichment, and network regulation analyses were used to analyze the data generated by high-throughput sequencing. Next, RMECs were subjected to HG (25 mM) conditions to induce RMECs apoptosis in vitro. A series of experiments, such as Transwell, the Scratch wound, and tube formation, were conducted to explore the regulatory effect of circRNA on RMECs. Fluorescence in situ hybridization (FISH), immunofluorescence staining, and Western blot were used to study the mechanism underlying circRNA-mediated regulation.

Results: A total of 53 differentially expressed circRNAs were found in patients with DR. Among these, hsa_circ_0000880 was significantly upregulated in both the diabetic epiretinal membranes and in an in vitro DR model of HG-treated RMECs. Hsa_circ_0000880 knockout facilitated RMECs vitality and decreased the paracellular permeability of RMECs under hyperglycemia. More importantly, silencing of hsa_circ_0000880 significantly inhibited HG-induced ROS production and RMECs apoptosis. Hsa_circ_0000880 acted as an endogenous sponge for eukaryotic initiation factor 4A-III (EIF4A3). Knockout of hsa_circ_0000880 reversed HG-induced decrease in EIF4A3 protein level.

Conclusions: Our findings suggest that hsa_circ_0000880 is a novel circRNA can induce RMECs apoptosis in response to HG conditions by sponging EIF4A3, offering an innovative treatment approach against DR.

Translational Relevance: The circRNAs participate in the dysregulation of microvascular endothelial function induced by HG conditions, indicating a promising therapeutic target for DR.

Introduction

Diabetic retinopathy (DR) has been established as the most prevalent type of diabetic vascular complication and a major cause of vision impairment in adults.[1] With the aging population, the number of individuals affected by DR is expected to rise significantly, making it a crucial global health concern.[2] The initial stage of DR is characterized by a gradual decline in vascular cells and the breakdown of intervascular junctions, leading to vascular leakage and

retinal edema.[3–5] It is widely acknowledged that DR is a microvascular disease, with retinal vessels being early and prominent targets of diabetes-associated injury.[6,7] Regrettably, effective treatments for the early damage of retinal vessels have not yet been established.

Endothelial cells (ECs), the fundamental units of retinal vascular structure, act as a physical barrier between blood and the surrounding tissue and play a vital role in maintaining vascular integrity.[8] Extensive research indicates that the earliest injuries in the early events of DR occur in retinal microvascular endothelial cells (RMECs), characterized by the disruption of the retinal blood barrier and the accumulation of leukocytes. It is now understood that high glucose (HG) levels during diabetes have been associated with metabolic disorders and represent the direct cause of RMEC injury. Failure to promptly correct these disorders may lead to apoptosis of RMECs and eventual development of the characteristic pathological alterations seen in nonproliferative DR.[9] The suppression of RMECs apoptosis offers a promising approach for DR treatment.[10–14] For example, Kim et al. found that HG induced Rab20 upregulation and reducing Rab20 expression could prevent HG-induced vascular cell death associated with DR.[10] Therefore, effective intervention strategies are urgently needed to target the primary RMECs injury at the early stages of DR.

Apoptosis of RMECs due to hyperglycemia involves multiple pathways, including autophagy, caspase-dependent apoptosis triggered by cytochrome c, somatic (CYCS) release, and various inflammatory pathways.[15] Circular RNAs (circRNAs) constitute a novel class of noncoding RNAs formed by back-splicing pre-mRNA transcripts. They play crucial post-transcriptional regulatory roles in the pathogenesis of various diseases, particularly cancers.[16–19] There is a growing consensus suggesting that circRNAs also have crucial regulatory functions in DR development and could serve as potential markers for diagnosing and treating DR.[20–22] Several circRNAs, such as CircDNMT3B, cZNF609, and CircHIPK3, have been implicated in retinal vascular dysfunction in a diabetic environment.[21] In a previous research, we documented hsa_circ_0001953 is upregulated in cases of proliferative DR (PDR) and has huge prospects for early diagnosis of this disease.[23] Thus, further investigation of the role of circRNAs in DR is warranted.

The RNA-binding protein (RBP) eukaryotic initiation factor 4A-III (eIF4A3, also known as DDX48) belongs to the eIF4A family and is involved in different post-transcriptional regulatory processes.[24,25] EIF4A3 is a critical component of RNA splicing. There is a rich literature available substantiating that certain circRNAs have the ability to function as molecular sponges for eIF4A3, affecting RNA localization, processing, transport, or stability. For instance, hsa_circ_0030042 was found to be downregulated in coronary heart disease, but its overexpression acted as an endogenous eIF4A3 sponge to inhibit abnormal autophagy in human umbilical vein endothelial cells.[26] Another research suggested eIF4A3 could bind to MMP9 mRNA, promoting circMMP9 circularization and expression in glioblastoma multiforme.[27] However, little is currently known on whether circRNAs sponge eIF4A3 or participate in RMEC apoptosis during the preliminary stages of DR.

Herein, we examined the expression profile of circRNAs in fibrovascular membranes from individuals diagnosed with PDR and who had undergone pars plana vitrectomy (PPV) surgery. We found that hsa_circRNA_0000880 was markedly upregulated in fibrovascular membranes of patients with PDR and an in vitro model of HG-induced RMECs injury. Subsequently, we investigated the role and underlying mechanism of hsa_circRNA_0000880 in HG-induced RMECs injury. These findings enhance our comprehension of how circular RNAs participate in the apoptosis of RMECs during the progression of DR, providing potential insights into strategies for early treatment of DR.

Materials and Methods

Ethics Approval

The study was conducted in accordance with the principles of the Declaration of Helsinki for research involving human subjects. Approval was also granted by the Ethics Committee of Qilu Hospital of Shandong University (Ethical approval number: KYLL-202111-024-1). All subjects provided informed consent prior to their inclusion in the study.

For this investigation, we consecutively enrolled 10 individuals diagnosed with type 2 diabetes (T2D) with PDR and 10 age and gender-matched nondiabetic patients with idiopathic macular epiretinal membrane who underwent PPV at the Department of Ophthalmology, Qilu Hospital of Shandong University. All included cases underwent 25-gauge PPV, and the preretinal membranes were dissected from the retinal surface using microsurgical forceps.[28] Following excision, all tissues were immersed in RNA later stabilization solution (Thermo Fisher) and promptly frozen at −80°C.

RNA Extraction and Quantitative Reverse Transcription Polymerase Chain Reaction

RNA was extracted from the samples using Trizol (Life Technologies Invitrogen Co., Carlsbad, CA, USA) as described in the kit's protocol. The concentration of total RNAs was determined using a spectrophotometer (NanoDrop ND-1000; Thermo Fisher Scientific, Waltham, MA, USA), and the integrity of total RNA was assessed using standard denaturing agarose gel electrophoresis. The RNA purity was evaluated by the A260/A280 absorbance ratio, with a ratio between 1.8 and 2.1, indicating ideal RNA integrity.

Total RNAs were then subjected to reverse transcription using a reagent kit (TaKaRa, Dalian, China) as recommended by the manufacturer. Polymerase chain reaction (PCR) assays were carried out using the commercial premix (SYBR Premix Ex Taq; TaKaRa) in the sequence detection system (ABI Prism 7300; Applied Biosystems, Foster City, CA, USA) to achieve the amplification reactions and obtain cycle threshold (CT) values. Each experiment had a total reaction volume of 20 µL, with 3 replicates per group, and the experiments were repeated thrice. The specificity of the PCR products was assessed using the dissociation curve. Glyceraldehyde 3-phosphate dehydrogenase (GAPDH) was used as an internal reference, and the relative expression of each sample was estimated according to the $2^{-\Delta\Delta Cq}$ method.

High Throughput Sequencing and Analysis

Four pairs of preretinal membranes were collected for circular RNA expression profiling. RNA high-throughput sequencing was conducted by Cloud-Seq Biotech (Shanghai, China) using total RNA. Initially, the rRNAs were removed with the NEBNext rRNA Depletion Kit (New England Biolabs, Inc., Ipswich, MA, USA). RNA libraries were constructed following the manufacturer's instructions, utilizing the NEBNext Ultra II Directional RNA Library Prep Kit (New England Biolabs, Inc., Ipswich, MA, USA). Quality control and quantification of libraries were performed using the BioAnalyzer 2100 system (Agilent Technologies, Inc., Santa Clara, CA, USA). The libraries were then sequenced on an Illumina Novaseq instrument with 150 base pair (bp) paired-end reads.

Paired-end reads were obtained from the Illumina NovaSeq 6000 sequencer and subjected to quality control with a Q30 threshold. Subsequently, the reads underwent 3' adaptor-trimming and removal of low-quality reads using Cutadapt (version 1.9.3). The high-quality reads were aligned to the reference genome/transcriptome using STAR (version 2.5.1b), and circular RNAs were detected using DCC (version 0.4.4). Data normalization was performed with edgeR (version 3.16.5). Differentially expressed circRNAs (DEcircRNAs) were identified through a *t*-test between the two groups. CircRNAs exhibiting fold changes (FCs) $\geq$ 2.0 and an adjusted *P* value (false discovery rate [FDR]) $\leq$ 0.15 were considered differentially expressed. Subsequently, functional enrichment analysis, including gene ontology (GO) and Kyoto Encyclopedia of Genes and Genomes (KEGG) pathway analyses, were conducted on the differentially expressed circRNA-associated genes. Significant GO terms and KEGG pathways were identified through the utilization of Fisher's exact test, accompanied by FDR correction applied to the *P* values. Statistical significance was considered for *P* values below 0.05. The circRNA-miRNA interactions were predicted using widely used target prediction software. The proprietary software, built upon Targetscan, was utilized to obtain putative miRNA binding sites and target mRNAs. Finally, a regulatory network was generated by Cytoscape (version 3.6.1), revealing the top five putative miRNAs that could bind to the circRNAs.

Cell Culture

Primary human RMECs were obtained from the Neuromics (Edina, MN, USA; Catalog Number: HEC09) and cultured in endothelial cell medium (Sciencell, Carlsbad, CA, USA) supplemented with 10% fetal bovine serum (FBS; Gibco) and 100 µg/mL penicillin/streptomycin (Gibco). The RMECs were cultured in a 37°C humidified incubator with 5% carbon dioxide in air.

Cell Transfection

The synthetic si-hsa_circ_0000880 (target sequences: 5′-CAAAATTGAAAAGT TGTCG-3′, riboFECT CP Reagent) and negative control si-hsa-circ_0000880 were procured from RiboBio (Guangzhou, China). When RMECs reached approximately 60% confluence, they were transfected with si-hsa_circ_0000880 or negative control si-hsa_circ_0000880 following the manufacturer's recommendations. After 24 hours post-transfection, the RMECs were exposed to hyperglycemic conditions (25 mM of d-glucose) for the indicated time. Control wells were treated with 5 mM d-glucose.[29–31] The experimental groups included: (1) the normal glucose (NG) group, (2) the HG group, (3) the HG+ si-hsa_circ_0000880 (HG+Si-circRNA) group, and (4) the HG+ negative control si-hsa _circ_0000880 (HG+Si-NC) group. Transfection efficiency was evalu-

ated by quantitative reverse transcription polymerase chain reaction (qRT-PCR) after 24 hours.

MTT Assay

Cell viability in different groups was assessed using the 3-(4, 5-dimethylthiazol-2-yl)-2, 5-diphenyltetrazolium-bromide assay (MTT) following the manufacturer's protocol. RMECs were cultivated in 96-well plates, with an approximate seeding density of 1×10^4 cells per well. After 48 hours of HG treatment and transfection, 5 mg/mL of MTT solution was added to each well and incubated for 3 hours at 37°C. Subsequently, 150 µL of dimethyl sulfoxide (DMSO) solution (100 mM, Sigma-Aldrich) was added to each well, and the optical density values at 490 nm wavelength were measured under spectrophotometry.

Scratch Assay

RMECs at a density of 2×10^5 cells/well were cultured in a 12-well plate and allowed to incubate until they reached confluence. The monolayer was then scratched using the tip of a 200 µL pipette, and the cells were washed with phosphate-buffered saline (PBS) to remove detached cells. Images of the same area were captured at 0 and 12 hours. The closure area of the wound was calculated using the formula: migration area (%) = $(A_0\text{-}A_n)/A_0 \times 100$, where A_0 represents the initial wound area, and A_n represents the remaining wound area at the measured time point.

Cell Migration Assay

RMECs were incubated under different conditions for 24 hours before performing the Transwell assay. Subsequently, the RMECs were placed into the upper chamber of Transwell 24-well plates (Corning, NY, USA) with 8 µm pore filters. After 12 hours, the cells attached to the upper chamber were removed, and the cells on the lower surface were fixed with 0.5% crystal violet for 10 minutes at room temperature. After being washed and air-dried, stained cells in three randomly selected fields were photographed and quantified under light microscopy (Olympus, Tokyo, Japan; magnification × 100).

Tube Formation Assay

Growth factor reduced Matrigel (BD Biosciences, Franklin Lakes, NJ, USA) was plated in 96-well plates and incubated at 37°C to gel for 30 minutes. After incubation under different conditions for 24 hours, RMECs (2×104 cells/well) were added to the polymerized Matrigel in the plates. After being incubated at 37°C for a duration of 3 hours, the tube formation process was assessed under bright-field microscopy. The total branching points and total number of tube-like structures were calculated using Image Pro Plus software (version 6.0; Media Cybernetics, Rockville, MD, USA).

Quantification of Intracellular Reactive Oxygen Species

The expression levels of intracellular reactive oxygen species (ROS) were examined using an ROS assay kit (Applygen Co. Ltd., Beijing, China) following the manufacturer's instructions. After treatment, the cells were incubated with 10 µM 2′, 7′-dichlorofluorescein diacetate (DCFH-DA) for 30 minutes at 37°C in the dark. ROS production was then assessed using a fluorescent microscope (Nikon, Tokyo, Japan) at different excitation (480 nm) and emission (525 nm) wavelengths. Three randomly selected fields were photographed, and the ROS fold was calculated based on the mean fluorescence intensities determined using ImageJ software.

Terminal Deoxynucleotidyl Transferase dUTP Nick End Labeling Assay

The TUNEL assay was performed using the In Situ Cell Detection Kit (Roche Applied Science) following the kit instructions. Three randomly selected fields were photographed under a fluorescence microscope, and the number of TUNEL-positive cells was quantified using ImageJ software. The percentage of apoptotic cells was calculated as the ratio of TUNEL-positive cells to the total number of cells.

Western Blot Analysis

Different groups of RMECs were lysed on ice using RIPA buffer. The protein lysates were then separated on 10% SDS polyacrylamide gels, followed by transfer onto PVDF membranes (Millipore, Bedford, MA, USA), and blocking with 5% skim milk. Primary antibodies, anti-eIF4A3 (Abcam, #ab32485, 1:1000), and anti-β-actin (Abcam, #ab8226, 1:1000), were added and incubated overnight at 4°C. Subsequently, secondary antibodies (1:1000; Millipore, USA) were incubated for 1 hour. Data were obtained and analyzed using ImageJ software.

Fluorescence In Situ Hybridization

To observe the location of hsa_circ_0000880 in RMECs, we performed FISH using a Fluorescent In situ Hybridization Kit (RiboBio, Guangzhou, China). Digoxin-labeled probes (Dig-5′-CCCCGACA ACTTTTCAATTTTGATCTC-3′-Dig) specific to hsa_circ_0000880 were designed and synthesized by Geneseed Biotech. Briefly, samples were fixed and pretreated with 4% paraformaldehyde (PFA) and PBS with 0.5% Triton X-100. Then, the hsa_circ_0000880 Probe Mix was used to hybridize with the samples at 37°C overnight. Finally, after 4,6-Diamidino-2-Phenylindole (DAPI) staining of the nuclei, the slides were imaged using a fluorescence microscope (NIKON Eclipse CI).

Immunofluorescence Staining

Cells fixation was conducted with 4% PFA for 30 minutes at room temperature. After 3 washes with PBS, the cells underwent a 10-minute treatment with PBS containing 0.2% Triton X-100. After blockade for 1 hour, the cells were stained with the primary antibody anti-eIF4A3 (Abcam, #ab32485, 1:100) at 4°C overnight. On the second day, after being washed 3 times with PBS, the cells were stained with the conjugated secondary antibody (1:100, Goat Anti-Rabbit IgG-FITC; Thermo Fisher Scientific, Inc.) for 1 hour at normal ambient temperature. Stained cells were visualized with a fluorescence microscope (NIKON Eclipse CI).

Statistical Analysis

GraphPad Prism 5.0 (Graph Pad Software, San Diego, CA, USA) was utilized for conducting statistical analysis and visualizing the data. The data were expressed as means ± standard error of the mean (SEM). To compare two groups of independent samples, the Student's *t*-test or Mann-Whitney test was used, as appropriate. For categorical variables, Fisher's exact test or the chi-square test was performed. Statistical significance was determined when the *P* value was less than 0.05.

Results

Clinical Characteristics of Subjects

The PDR group included 10 patients (5 men and 5 women) with a mean age of 60.0 ± 1.93 years, and the control group consisted of 10 patients (5 men and 5 women) with a mean age of 62.4 ± 1.58 years. Both groups did not differ significantly in age ($P = 0.348$). In the patients with PDR, the average duration of diabetes was 15.1 ± 1.52 years.

DECircRNAs in the Epiretinal Membranes Between Patients With PDR and Non-Diabetic Patients

A high throughput circRNA microarray was utilized to investigate the differences in circRNA expression profiles in the epiretinal membranes between PDR and nondiabetic patients. The microarray cohort included four patients with PDR and four nondiabetic patients with idiopathic macular epiretinal membranes. Based on an FC value greater than 2.0 and FDR ≤ 0.15, we identified 53 DEcircRNAs, including 16 upregulated and 37 downregulated circRNAs. Hierarchical clustering analysis revealed distinct expression patterns of circular RNAs across the samples (Fig. 1A).

Bioinformatic Analysis for Upregulated Expressed CircRNAs

Given that circRNAs generally exhibit low expression and upregulated circRNAs reportedly play significant roles in the development of DR, we focused solely on the upregulated circRNAs. To better comprehend the role of the identified upregulated circRNAs, we conducted functional enrichment analysis on the host genes of circRNAs. The most significantly enriched GO terms in terms of biological process (BP), cellular component (CC), and molecular function (MF) were organelle organization, post-mRNA release spliceosomal complex, and 1-phosphatidylinositol-3-kinase activity, respectively (Fig. 1B). KEGG pathway analysis suggested these circRNAs might participate in 10 signaling pathways, including axon guidance, endocytosis, and regulation of actin cytoskeleton (Fig. 1C).

CircRNAs are competitive endogenous RNAs that function as microRNA sponges and can bind to RBPs to regulate gene transcription. To better understand the regulatory role of these upregulated circRNAs, we performed circRNA-miRNA and circRNA-protein interactions using Targetscan and CircInteractome. The results demonstrated a complex regulatory network, with these circRNAs interacting with various miRNAs and RBPs. Each circRNA had multiple direct binding sites for miRNAs, and numerous RBPs were found to bind to circRNAs. Some RBPs, particularly EIF4A3, HuR, and FUS, were implicated in different binding proteins (BPs), such as regulating cell proliferation, differentiation, migration, and apoptosis.[27,32,33]

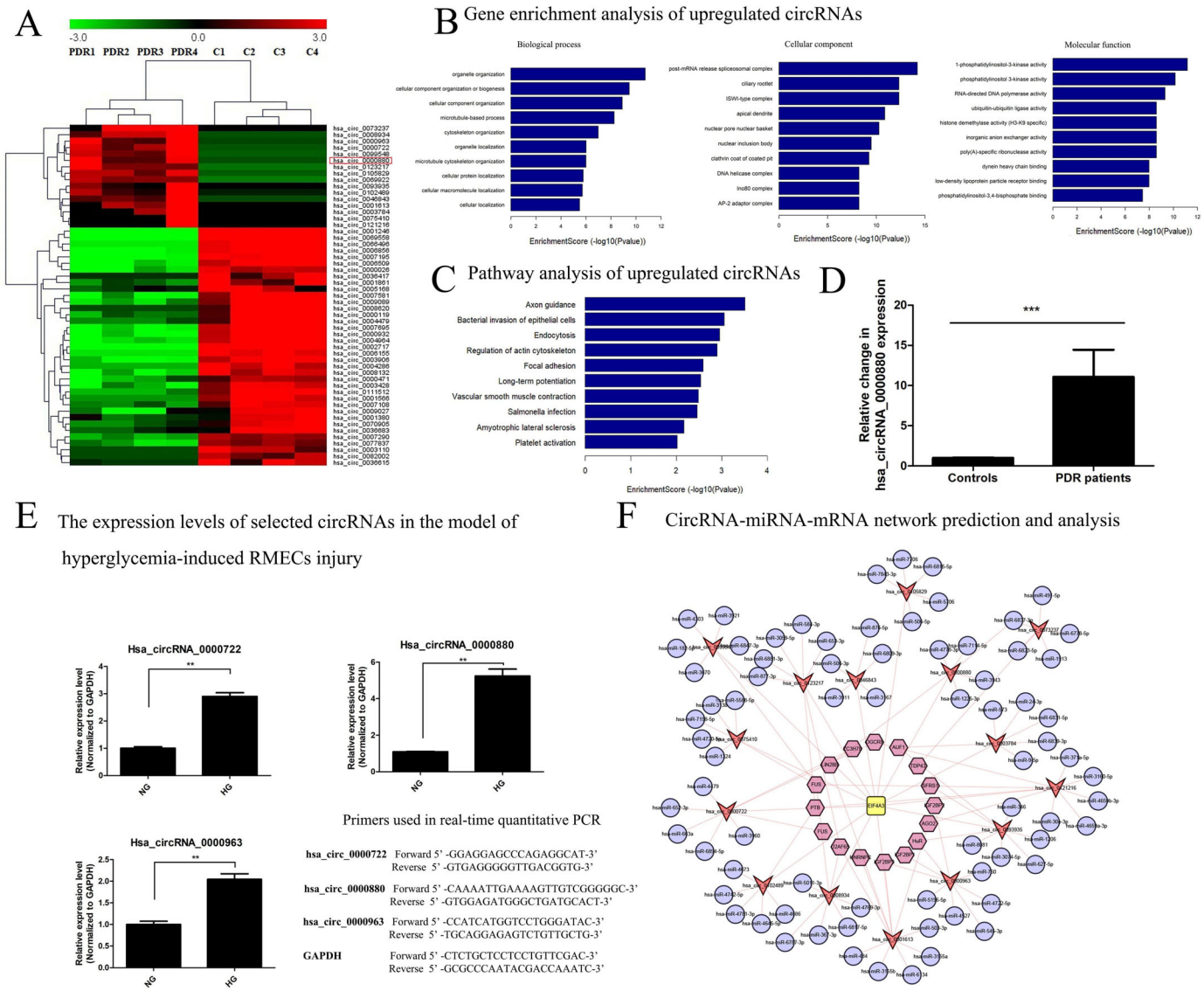

Figure 1. Identification of differentially expressed circRNAs in the epiretinal membranes between patients with PDR and nondiabetic patients. (**A**) The heatmap was constructed to compare expression of circRNAs between patients with PDR and nondiabetic patients. High expression is indicated in *red* and low expression is indicated in *green*. (**B, C**) GO annotation enrichment analysis and KEGG pathway analysis of the upregulated circRNAs. The vertical axis is the description of GO terms and the horizontal axis is the enrichment score (-log10 [*P* value]) of the pathways. (**D**) Validation of hsa_circ_0000880 by qRT-PCR in the epiretinal membranes between patients with PDR and nondiabetic patients. (**E**) The qRT-PCR analysis of three circRNAs expression in the vitro model of hyperglycemia-induced RMECs injury. The relative expression levels were normalized to the expression of GAPDH. (**F**) CircRNA-miRNA interactions and circRNA-protein interactions were constructed using Cytoscape. The *light blue circles* represent miRNAs. The *red triangles* represent differentially expressed circRNAs. The *red hexagons* represent circRNA-targeted proteins. The *yellow square* represents EIF4A3. The values are expressed as the means ± SEMs. $^{**}P < 0.01$, $^{***}P < 0.001$. PDR, proliferative diabetic retinopathy; GO, Gene Ontology; KEGG, Kyoto Encyclopedia of Genes and Genomes.

Hsa_circ_0000880 Was Highly Expressed in PDR Epiretinal Membranes and High Glucose-Stimulated RMECs

Previous studies have identified ECs as the main cell type in the PDR epiretinal membranes.[34] To establish an in vitro DR model of endothelial cells, the RMECs were treated with HG, and RT-qPCR was used to quantify the three upregulated circular RNAs (CircRNAID < 1000). Among them, hsa_circ_0000880 showed the most significant induction in cells treated with HG (Fig. 1E). To investigate whether hsa_circ_0000880 is upregulated in PDR epiretinal membranes, we collected samples from PDR ($n = 6$) and non-DM ($n = 6$) cases with idiopathic macular epiretinal membrane. Hsa_circ_0000880 expression was upregulated in PDR cases compared to nondiabetic cases, consistent with

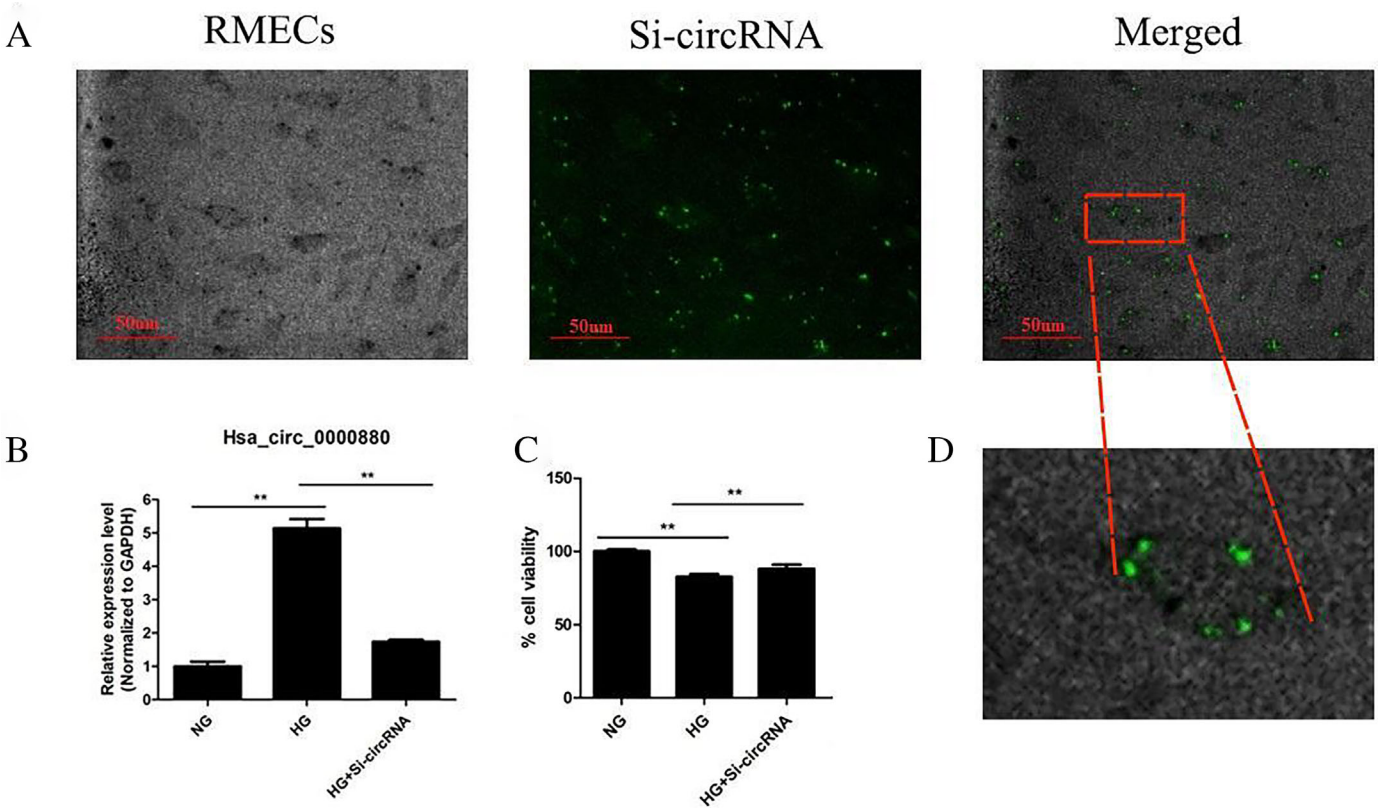

Figure 2. The effect of hsa_circ_0000880 silencing on the viability of RMECs. (**A**) RMECs were transiently transfected with hsa_circ_0000880 siRNA for 24 hours. (**B**) Relative expression level of has_circ_0000880 in the NG, the HG, and the HG+Si-circRNA groups. (**C**) MTT assay showed the cell viability in the NG, the HG, and the HG+Si-circRNA groups. (**D**) Representative image of RMECs after siRNA transfection. The values are expressed as the means ± SEMs. $^{**}P < 0.01$. RMECs, retinal microvascular endothelial cells; HG, high glucose.

the microarray data (Fig. 1D). These findings demonstrated the upregulation of hsa_circ_0000880 in PDR samples and HG-treated RMECs.

Hsa_circ_0000880 Regulated RMECs Function Under HG Conditions In Vitro

Next, we assessed the regulatory role of hsa_circ_0000880 in RMECs function under in vitro HG conditions. We used 3 different siRNAs to silence hsa_circ_0000880 expression. The siRNA1 transfection successfully downregulated hsa_circ_0000880 expression at 24 hours post-transfection (Fig. 2A, 2B).

Subsequently, we investigated the effect of hsa_circ_0000880 on RMEC proliferation, migration, and tube formation. MTT assay revealed that HG treatment significantly inhibited cell proliferation of RMECs, whereas hsa_circ_0000880 silencing promoted cell proliferation (Fig. 2C). Transwell migration and the scratch wound assays demonstrated that hsa_circ_0000880 silencing significantly increased RMEC migration under HG conditions (Fig. 3). To assess the integrity of the human retinal endothelial barrier under hyperglycemic conditions, we performed a tube formation assay after HG treatment and hsa_circ_0000880 silencing. HG treatment increased the paracellular permeability of RMECs, which was mitigated by hsa_circ_0000880 knockdown (Fig. 4).

Hsa_circ_0000880 Silencing Inhibited HG-Induced ROS Production and Apoptosis of RMECs

Current evidence suggests that HG can increase intracellular ROS formation, which is the main mechanism leading to the dysregulation of endothelial cells. Excess ROS can be toxic and linked to cell apoptosis.[35–37] Therefore, we explored the impact of inhibiting hsa_circ_0000880 on ROS generation and apoptosis in RMECs after HG treatment. As depicted in Fig. 5, HG treatment significantly increased ROS accumulation in RMECs, whereas hsa_circ_0000880 silencing notably reduced ROS levels in RMECs. Additionally, we conducted a TUNEL assay and observed that hsa_circ_0000880 silencing had a mitigating effect on

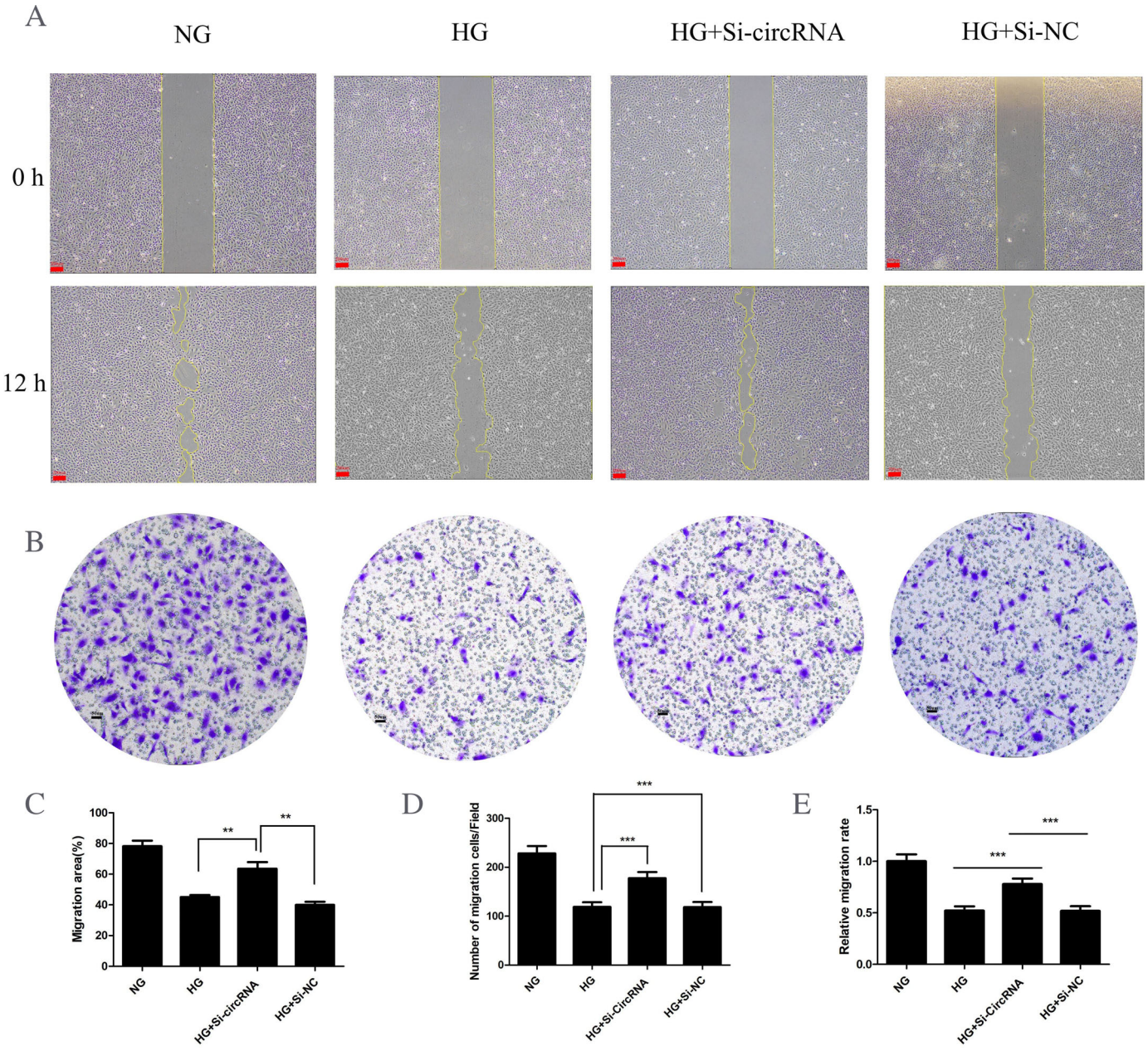

Figure 3. The effect of hsa_circ_0000880 on the wound healing and cell migration of RMECs under hyperglycemic conditions. (**A**) The scratch wound assay in the NG, the HG, the HG+Si-circRNA, and the HG+Si-NC groups (scale bar = 200 µm). (**B**) Transwell assay in the NG, the HG, the HG+Si-circRNA, and the HG+Si-NC groups (scale bar = 50 µm). (**C**) The migration area in the scratch wound assay. (**D**) The number of migration cells per field in the Transwell experiment. (**E**) Relative migration rate in the Transwell experiment. The values are expressed as the means ± SEMs. $^{**}P < 0.01$, $^{***}P < 0.001$. RMECs, retinal microvascular endothelial cells; HG, high glucose.

the apoptosis of RMECs induced by HG treatment (see Fig. 5A).

Hsa_circ_0000880 Regulated RMECs Function by Targeting EIF4A3

CircRNAs are widespread in mammals and regulate genes at transcriptional and post-transcriptional levels through various mechanisms.[18] To gain a deeper understanding of the mechanism of hsa_circ_0000880, its subcellular location in RMECs was probed. The fluorescence in situ hybridization (FISH) analysis demonstrated that the main localization of hsa_circ_0000880 was within the nucleus, suggesting a potential role as a protein sponge (Fig. 6C). To identify potential RBPs that interact with hsa_circ_0000880, we conducted a circRNA-RBP interaction network prediction using the Circinter-

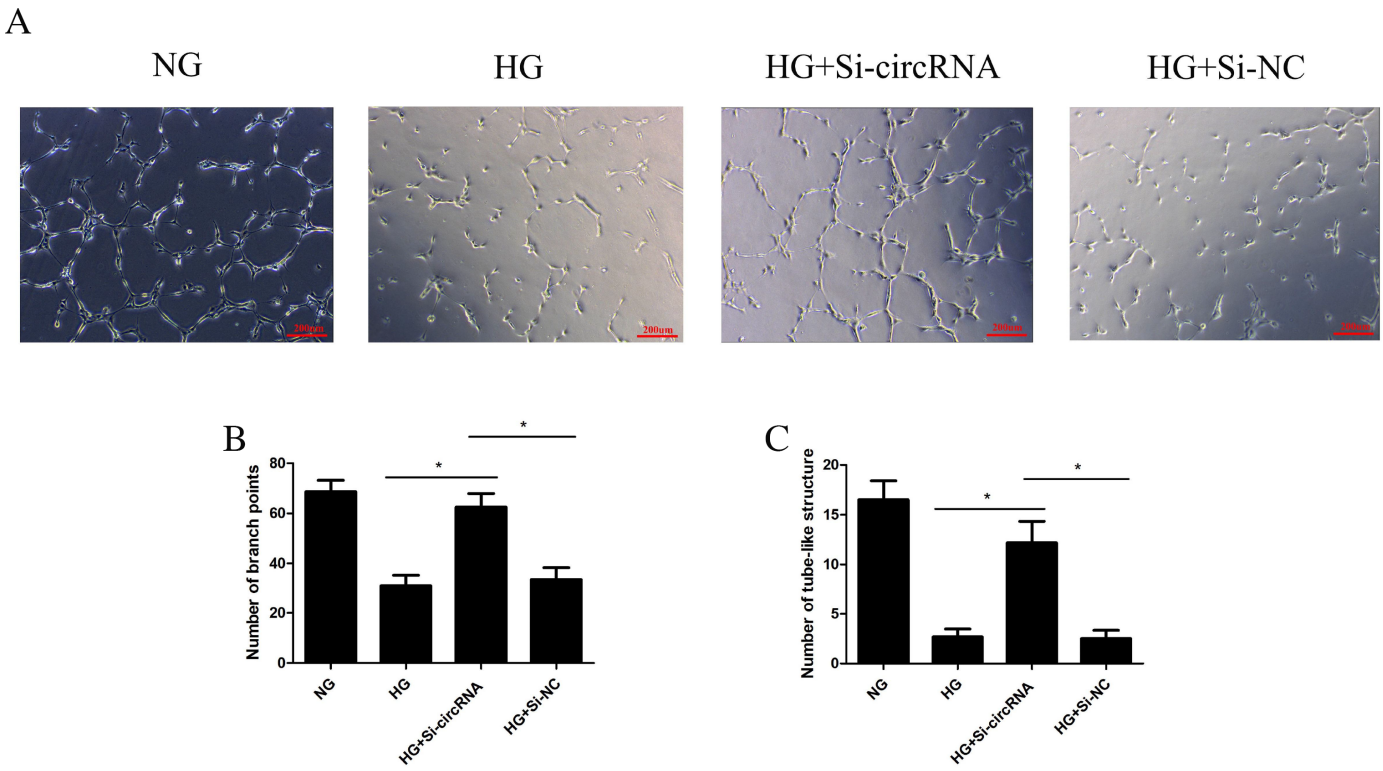

Figure 4. The effect of hsa_circ_0000880 on the tube formation of RMECs under hyperglycemic conditions. (**A**) Tube networks formation of RMECs in the NG, the HG, the HG+Si-circRNA, and the HG+Si-NC groups. (**B**) Number of branch points in the NG, the HG, the HG+Si-circRNA, and the HG+Si-NC groups. (**C**) Number of tube-like structures in the NG, the HG, the HG+Si-circRNA, and the HG+Si-NC groups. The values are expressed as the means ± SEMs. *$P < 0.05$. RMECs, retinal microvascular endothelial cells; HG, high glucose. Scale bar = 200 µm.

actome database (Fig. 1F). Based on our prediction, it was suggested that hsa_circ_0000880 could potentially interact with EIF4A3. This interaction between hsa_circ_0000880 and EIF4A3 involved 3 major RNA regions (0-263, -4-24, and -599–551 nucleotides) and 4 domains (25-114, 37-114, 2-28, and 3-49 amino acids) of the EIF4A3 protein (Fig. 6B). The FISH analysis and immunofluorescence staining further confirmed the colocalization of hsa_circ_0000880 with EIF4A3 in RMECs (see Fig. 6C). To confirm the regulatory influence of EIF4A3 on cell functions mediated by hsa_circ_0000880, we conducted Western blot analysis. The protein expression of EIF4A3 was markedly lower in the HG group than in the NG group. Moreover, hsa_circ_0000880 silencing effectively reversed the HG-induced decrease in the EIF4A3 protein level (Fig. 6D).

Discussion

DR is a multifactorial disease, and its development involves a complex pathological process. The pathogenesis of DR remains not fully understood.[6,38] Recently, circRNAs have gained more attention, given their potential functions in the pathogenesis of DR. However, few circRNAs with well-established biological functions in DR have been documented.[20,39,40] Therefore, exploring new functions and mechanisms of circRNAs is essential. Herein, we investigated the disparities in circRNA profiles within epiretinal membranes between PDR and nondiabetic cases. Fifty-three DEcircRNAs were found in patients with PDR. Among these, hsa_circ_0000880 exhibited significant upregulation in both PDR epiretinal membranes and in vitro DR models of HG-treated RMECs. We further demonstrated that hsa_circ_0000880 could regulate RMECs function under HG conditions in vitro by targeting EIF4A3, suggesting its potential importance in DR development.

The role of circRNAs in different human diseases, including DR, has emerged as a novel research hotspot.[18] The aberrant growth of blood vessels in the retina is a critical factor leading to irreversible blindness, as observed in PDR. Emerging evidence indicates that circRNAs are essential in angiogenesis.[39–43] CircRNA HIPK3 (CircHIPK3) exhibited significant upregulation in diabetic retinas and retinal ECs after treatment with diabetes-related

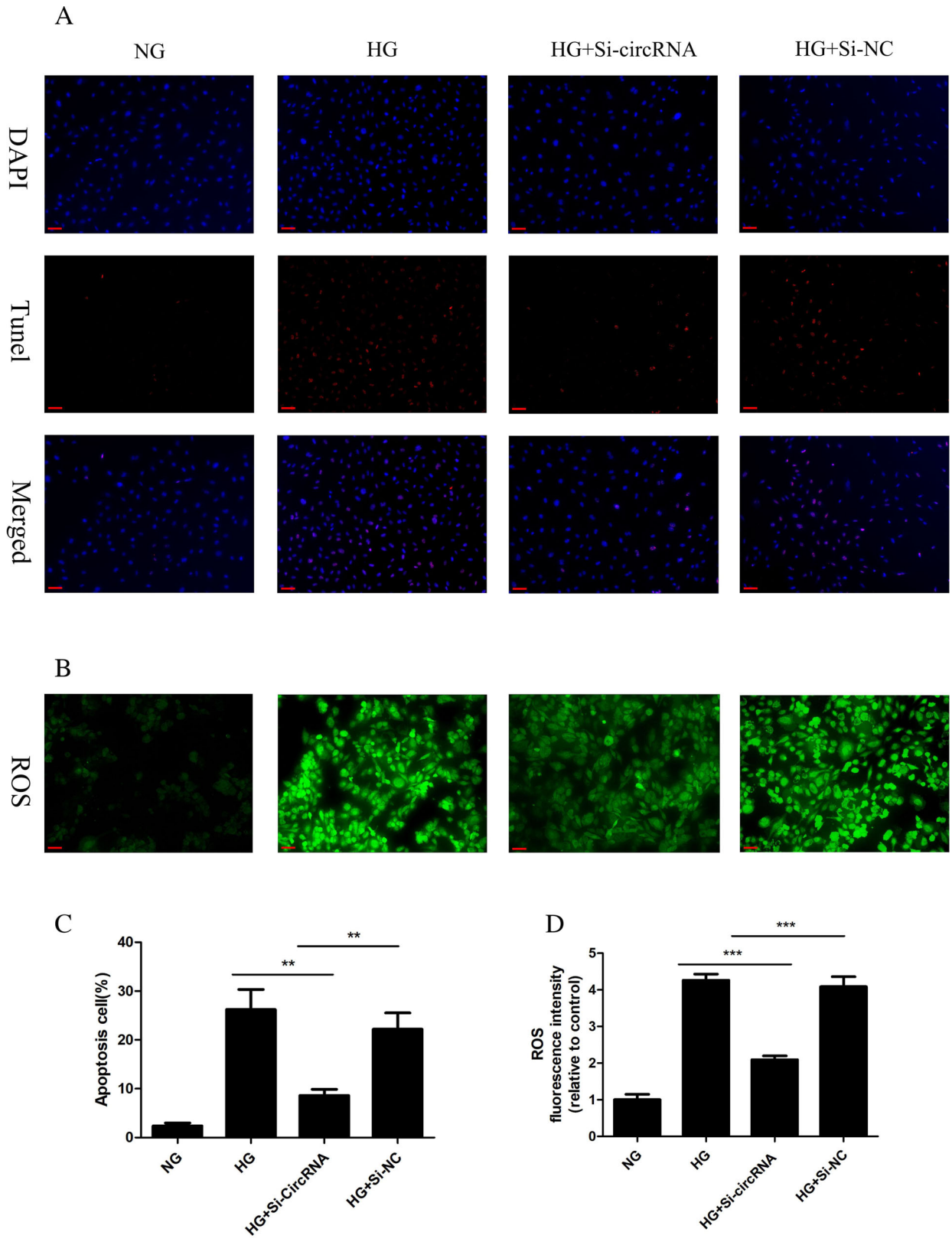

Figure 5. Hsa_circ_0000880 silencing decreased the production of HG-induced ROS and suppressed the apoptosis of RMECs under HG conditions. (**A**, **C**) Cell apoptosis was determined by TUNEL assay. (**B**, **D**) Intracellular ROS quantities were assessed using DCFH-DA staining. The values are expressed as the means ± SEMs. $^{**}P < 0.01$, $^{***}P < 0.001$. HG, high glucose; ROS, reactive oxygen species; RMECs, retinal microvascular endothelial cells; DCFH-DA, dichlorodihydrofluorescein diacetate; TUNEL, Terminal deoxynucleotidyl transferase dUTP nick end labeling. Scale bar = 50 µm.

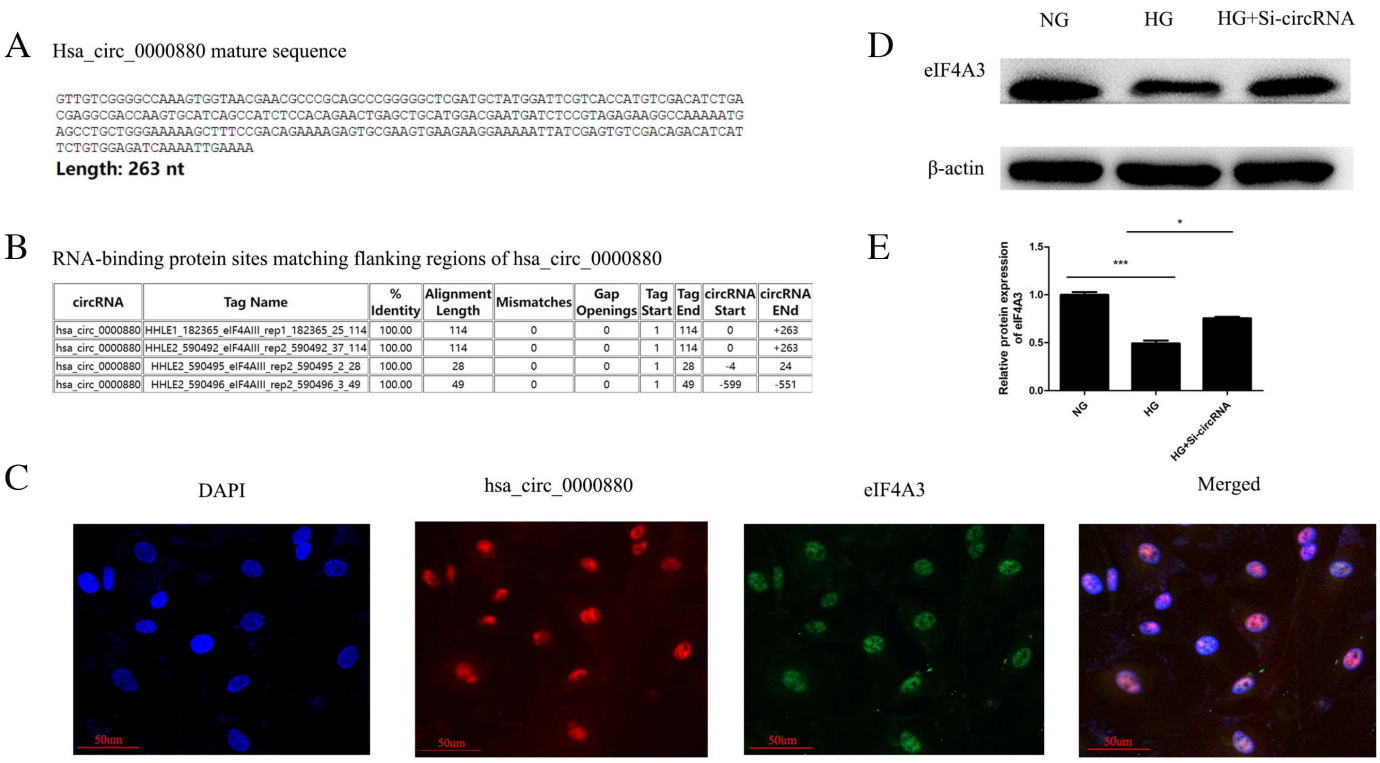

Figure 6. Hsa_circ_0000880 localized in the nucleus and interact with EIF4A3. (**A**) Mature sequence of hsa_circ_0000880. (**B**) Matching flanking regions for hsa_circ_0000880-EIF4A3 binding. (**C**) FISH images showing that hsa_circ_0000880 was mostly located in the nucleus and co-localized with EIF4A3 in RMECs. (**D**, **E**) The relative protein expression of EIF4A3 in HG-treated and hsa_circ_0000880 knockdown RMECs. The values are expressed as the means ± SEMs. $^{*}P < 0.05$, $^{***}P < 0.001$. RMECs, retinal microvascular endothelial cells; EIF4A3, eukaryotic initiation factor 4A-III; FISH, Fluorescence in situ hybridization assay.

stressors. Manipulating CircHIPK3 expression could alter endothelial cell function.[39] Besides, circRNA–PWWP2A (CPWWP2A) exhibited a clear increase in the retinas of diabetic mice and patients with diabetes. Silencing CPWWP2A notably rescued retinal vascular leakage and pericyte loss and reduced the number of microaneurysms and acellular vascular structures in a diabetic animal model.[40] Herein, we observed a specific upregulation of a novel circRNA, hsa_circ_0000880, in PDR epiretinal membranes. Reducing hsa_circ_0000880 expression stimulated RMECs to proliferate and migrate and form tube-like structures.

Current evidence suggests that hyperglycemia causes a surge in reactive oxygen species levels. HG-induced ROS overproduction is essential in DR development. There is a rich literature available substantiating that HG leads to the overproduction of ROS in endothelial cells, triggering apoptosis, and gradually altering the microvessel architecture in the retina, contributing to the development of initial lesions.[44–47] In our study, we confirmed that HG stimulation resulted in ROS synthesis, conducive to the apoptosis in RMECs. More importantly, we found that hsa_circ_0000880 silencing significantly decreased the expression of ROS and inhibited HG-induced apoptosis in RMECs. Our findings indicate that hsa_circ_0000880 is involved in HG-induced endothelial cell apoptosis and silencing hsa_circ_0000880 exerts protective effects against HG-induced vascular endothelial dysfunction. Taken together, our findings suggest that hsa_circ_0000880 regulates diabetic vascular dysfunction.

Recent research has unveiled various functions of circRNAs, such as acting as miRNA sponges, forming RNA-protein complexes by binding to RBPs and potentially enabling translation.[48] Most circRNAs are located in the cytoplasm, functioning as miRNA sponges. However, some circRNAs are retained in the nucleus and regulate cell activities by interacting with different proteins in related signaling pathways.[49] To investigate how hsa_circ_0000880 regulates RMECs under HG conditions, we initially observed its location in RMECs using FISH analysis, which revealed that hsa_circ_0000880 was highly expressed in the nucleus, indicating that it may function as a protein sponge. In light of this observation, we utilized the Circinteractome database to conduct a prediction of the circRNA-

RBP interaction network. Through this analysis, we identified EIF4A3 as a potential interacting protein with hsa_circ_0000880.

EIF4A3 is a component of the exon junction complex and is involved in different post-transcriptional regulatory processes, with elevated expression reported in cancers.[50–52] Reduced EIF4A3 expression has been associated with abnormal neural crest development and excessive cell death.[25,53] At the molecular level, the loss of EIF4A3 has been shown to impair cell viability and inhibit cell migration. Previous studies have revealed that certain circRNAs, acting as RBPs, can bind to EIF4A3 and regulate the expression of cell-cycle-regulatory genes at the translational or post-translational level.[26,27] Based on the results of our bioinformatic analysis, we hypothesized that hsa_circ_0000880 may also interact with EIF4A3. To test this hypothesis, we conducted FISH analysis and immunofluorescence staining, which confirmed the co-localization of hsa_circ_0000880 with EIF4A3 in RMECs. Moreover, silencing hsa_circ_0000880 significantly reversed the HG-induced decrease in EIF4A3 protein levels. For the first time, we had discovered that hsa_circ_0000880 could inhibit the translation of EIF4A3 by competitively binding to mRNA transcripts, thereby reducing protein translation rates. However, further experiments are warranted to better understand circRNA-mediated DR pathogenesis in the future.

In conclusion, hsa_circ_0000880 is a hitherto undocumented circular RNA that participates in the dysregulation of vascular endothelial function induced by HG conditions. Hsa_circ_0000880 exhibited significant upregulation in both PDR epiretinal membranes and an in vitro DR model of HG-treated RMECs. Importantly, hsa_circ_0000880 was shown to regulate RMECs' function by targeting EIF4A3 under HG conditions in vitro. This study provides important perspectives into the involvement of circular RNAs in DR progression, and targeting hsa_circ_0000880 may hold promise as an effective treatment strategy for DR.

Acknowledgments

Supported by Natural Science Foundation of Shandong Province (ZR2023MH139) and the grant from Shandong University (No. 6010220078).

Disclosure: **J. Wang**, None; **N. Yang**, None; **W. Li**, None; **H. Zhang**, None; **J. Li**, None

* JW and NY contributed equally to the work presented here and should therefore be regarded as equivalent authors.

References

1. Cheung N, Mitchell P, Wong TY. Diabetic retinopathy. *Lancet*. 2010;376(9735):124–136.
2. Dal Canto E, Ceriello A, Rydén L, et al. Diabetes as a cardiovascular risk factor: an overview of global trends of macro and micro vascular complications. *Eur J Prev Cardiol*. 2019;26:25–32.
3. Cerani A, Tetreault N, Menard C, et al. Neuron-derived semaphorin 3A is an early inducer of vascular permeability in diabetic retinopathy via neuropilin-1. *Cell Metab*. 2013;18:505–518.
4. Hu J, Dziumbla S, Lin J, et al. Inhibition of soluble epoxide hydrolase prevents diabetic retinopathy. *Nature*. 2017;552:248–252.
5. Roy S, Bae E, Amin S, Kim D. Extracellular matrix, gap junctions, and retinal vascular homeostasis in diabetic retinopathy. *Exp Eye Res*. 2015;133:58–68.
6. Wong TY, Cheung CM, Larsen M, Sharma S, Simó R. Diabetic retinopathy. *Nat Rev Dis Primers*. 2016;2:16012.
7. Song P, Yu J, Chan KY, Theodoratou E, Rudan I. Prevalence, risk factors and burden of diabetic retinopathy in China: a systematic review and meta-analysis. *J Glob Health*. 2018;8(1):010803.
8. Capitão M, Soares R. Angiogenesis and inflammation crosstalk in diabetic retinopathy. *J Cell Biochem*. 2016;117(11):2443–2453.
9. Beltramo E, Porta M. Pericyte loss in diabetic retinopathy: mechanisms and consequences. *Curr Med Chem*. 2013;20(26):3218–3225.
10. Kim D, Lewis CS, Sarthy VP, Roy S. High-glucose-induced Rab20 upregulation disrupts gap junction intercellular communication and promotes apoptosis in retinal endothelial and Müller cells: implications for diabetic retinopathy. *J Clin Med*. 2020;9(11):3710.
11. Kong H, Zhao H, Chen T, Song Y, Cui Y. Targeted P2X7/NLRP3 signaling pathway against inflammation, apoptosis, and pyroptosis of retinal endothelial cells in diabetic retinopathy. *Cell Death Dis*. 2022;13:336.
12. Hammer SS, Vieira CP, McFarland D, et al. Fasting and fasting-mimicking treatment activate SIRT1/LXRα and alleviate diabetes-induced systemic and microvascular dysfunction. *Diabetologia*. 2021;64:1674–1689.

13. Barber AJ, Gardner TW, Abcouwer SF. The significance of vascular and neural apoptosis to the pathology of diabetic retinopathy. *Invest Ophthalmol Vis Sci*. 2011;52:1156–1163.
14. Aires ID, Madeira MH, Boia R, et al. Intravitreal injection of adenosine A(2A) receptor antagonist reduces neuroinflammation, vascular leakage and cell death in the retina of diabetic mice. *Sci Rep*. 2019;9:17207.
15. Mrugacz M, Bryl A, Zorena K. Retinal vascular endothelial cell dysfunction and neuroretinal degeneration in diabetic patients. *J Clin Med*. 2021;10(3):458.
16. Li F, Yang Q, He AT, Yang BB. Circular RNAs in cancer: limitations in functional studies and diagnostic potential. *Semin Cancer Biol*. 2021;75:49–61.
17. van Zonneveld AJ, Kölling M, Bijkerk R, Lorenzen JM. Circular RNAs in kidney disease and cancer. *Nat Rev Nephrol*. 2021;17(12):814–826.
18. Verduci L, Tarcitano E, Strano S, Yarden Y, Blandino G. CircRNAs: role in human diseases and potential use as biomarkers. *Cell Death Dis*. 2021;12(5):468.
19. Seimiya T, Otsuka M, Fujishiro M. Roles of circular RNAs in the pathogenesis and treatment of pancreatic cancer. *Front Cell Dev Biol*. 2022;10: 1023332.
20. Zhang SJ, Chen X, Li CP, et al. Identification and characterization of circular RNAs as a new class of putative biomarkers in diabetes retinopathy. *Invest Ophthalmol Vis Sci*. 2017;58(14):6500–6509.
21. Zhou HR, Kuang HY. Circular RNAs: novel target of diabetic retinopathy. *Rev Endocr Metab Disord*. 2021;22(2):205–216.
22. Trotta MC, Gesualdo C, Platania C, et al. Circulating miRNAs in diabetic retinopathy patients: prognostic markers or pharmacological targets. *Biochem Pharmacol*. 2021;186:114473.
23. Wu Z, Liu B, Ma Y, Chen H, Wu J, Wang J. Discovery and validation of hsa_circ_0001953 as a potential biomarker for proliferative diabetic retinopathy in human blood. *Acta Ophthalmol*. 2021;99(3):306–313.
24. Miller EE, Kobayashi GS, Musso CM, et al. EIF4A3 deficient human iPSCs and mouse models demonstrate neural crest defects that underlie Richieri-Costa-Pereira syndrome. *Hum Mol Genet*. 2017;26(12):2177–2191.
25. Kanellis DC, Espinoza JA, Zisi A, et al. The exon-junction complex helicase eIF4A3 controls cell fate via coordinated regulation of ribosome biogenesis and translational output. *Sci Adv*. 2021;7(32):eabf7561.
26. Yu F, Zhang Y, Wang Z, Gong W, Zhang C. Hsa_circ_0030042 regulates abnormal autophagy and protects atherosclerotic plaque stability by targeting eIF4A3. *Theranostics*. 2021;11(11):5404–5417.
27. Wang R, Zhang S, Chen X, et al. EIF4A3-induced circular RNA MMP9 (circMMP9) acts as a sponge of miR-124 and promotes glioblastoma multiforme cell tumorigenesis. *Mol Cancer*. 2018;17(1):166.
28. Wang J, Gao X, Liu J, et al. Effect of intravitreal conbercept treatment on the expression of long noncoding RNAs and mRNAs in proliferative diabetic retinopathy patients. *Acta Ophthalmol*. 2019;97(6):e902–e912.
29. Ye EA, Steinle JJ. miR-146a suppresses STAT3/VEGF pathways and reduces apoptosis through IL-6 signaling in primary human retinal microvascular endothelial cells in high glucose conditions. *Vision Res*. 2017;139:15–22.
30. Nizamutdinova IT, Kim YM, Kim HJ, Seo HG, Lee JH, Chang KC. Carbon monoxide (from CORM-2) inhibits high glucose-induced ICAM-1 expression via AMP-activated protein kinase and PPAR-gamma activations in endothelial cells. *Atherosclerosis*. 2009;207:405–411.
31. Piga R, Naito Y, Kokura S, Handa O, Yoshikawa T. Short-term high glucose exposure induces monocyte-endothelial cells adhesion and transmigration by increasing VCAM-1 and MCP-1 expression in human aortic endothelial cells. *Atherosclerosis*. 2007;193:328–334.
32. Amadio M, Pascale A, Cupri S, et al. Nanosystems based on siRNA silencing HuR expression counteract diabetic retinopathy in rat. *Pharmacol Res*. 2016;111:713–720.
33. Brooke GN, Culley RL, Dart DA, et al. FUS/TLS is a novel mediator of androgen-dependent cell-cycle progression and prostate cancer growth. *Cancer Res*. 2011;71:914–924.
34. Hu Z, Mao X, Chen M, et al. Single-cell transcriptomics reveals novel role of microglia in fibrovascular membrane of proliferative diabetic retinopathy. *Diabetes*. 2022;71(4):762–773.
35. Calderon GD, Juarez OH, Hernandez GE, Punzo SM, De la Cruz ZD. Oxidative stress and diabetic retinopathy: development and treatment. *Eye (Lond)*. 2017;31:1122–1130.
36. Dehdashtian E, Mehrzadi S, Yousefi B, et al. Diabetic retinopathy pathogenesis and the ameliorating effects of melatonin; involvement of

autophagy, inflammation and oxidative stress. *Life Sci*. 2018;193:20–33.
37. Volpe C, Villar-Delfino PH, Dos Anjos P, Nogueira-Machado JA. Cellular death, reactive oxygen species (ROS) and diabetic complications. *Cell Death Dis*. 2018;9:119.
38. Platania C, Maisto R, Trotta MC, et al. Retinal and circulating miRNA expression patterns in diabetic retinopathy: an in silico and in vivo approach. *Br J Pharmacol*. 2019;176:2179–2194.
39. Shan K, Liu C, Liu BH, et al. Circular noncoding RNA HIPK3 mediates retinal vascular dysfunction in diabetes mellitus. *Circulation*. 2017;136(17):1629–1642.
40. Liu C, Ge HM, Liu BH, et al. Targeting pericyte-endothelial cell crosstalk by circular RNA-cPWWP2A inhibition aggravates diabetes-induced microvascular dysfunction. *Proc Natl Acad Sci USA*. 2019;116(15):7455–7464.
41. Balandeh E, Mohammadshafie K, Mahmoudi Y, et al. Roles of non-coding RNAs and angiogenesis in glioblastoma. *Front Cell Dev Biol*. 2021;9:716462.
42. Hernández-Romero IA, Guerra-Calderas L, Salgado-Albarrán M, Maldonado-Huerta T, Soto-Reyes E. The regulatory roles of non-coding RNAs in angiogenesis and neovascularization from an epigenetic perspective. *Front Oncol*. 2019;9:1091.
43. Ghaedrahmati F, Nasrolahi A, Najafi S, et al. Circular RNAs-mediated angiogenesis in human cancers. *Clin Transl Oncol*. 2023;25:3101–3121.
44. Giacco F, Brownlee M. Oxidative stress and diabetic complications. *Circ Res*. 2010;107(9):1058–1070.
45. Sada K, Nishikawa T, Kukidome D, et al. Hyperglycemia induces cellular hypoxia through production of mitochondrial ROS followed by suppression of aquaporin-1. *PLoS One*. 2016;11(7):e0158619.
46. Shah MS, Brownlee M. Molecular and cellular mechanisms of cardiovascular disorders in diabetes. *Circ Res*. 2016;118(11):1808–1829.
47. Qasim N, Arif A, Mahmood R. Hyperglycemia enhances the generation of ROS and RNS that impair antioxidant power and cause oxidative damage in human erythrocytes. *Biochem Cell Biol*. 2023;101(1):64–76.
48. Tang X, Ren H, Guo M, Qian J, Yang Y, Gu C. Review on circular RNAs and new insights into their roles in cancer. *Comput Struct Biotechnol J*. 2021;19:910–928.
49. Boon RA, Jaé N, Holdt L, Dimmeler S. Long noncoding RNAs: from clinical genetics to therapeutic targets. *J Am Coll Cardiol*. 2016;67(10):1214–1226.
50. Ito M, Iwatani M, Kamada Y, et al. Discovery of selective ATP-competitive eIF4A3 inhibitors. *Bioorg Med Chem*. 2017;25(7):2200–2209.
51. Iwatani-Yoshihara M, Ito M, Ishibashi Y, et al. Discovery and characterization of a eukaryotic initiation factor 4A-3-selective inhibitor that suppresses nonsense-mediated mRNA decay. *ACS Chem Biol*. 2017;12(7):1760–1768.
52. Zhu Y, Ren C, Yang L. Effect of eukaryotic translation initiation factor 4A3 in malignant tumors. *Oncol Lett*. 2021;21(5):358.
53. Mao H, McMahon JJ, Tsai YH, Wang Z, Silver DL. Haploinsufficiency for core exon junction complex components disrupts embryonic neurogenesis and causes p53-mediated microcephaly. *PLoS Genet*. 2016;12(9):e1006282.